

Effect of Heat treatment and Phase Change on BFS of Two Hydroxyapatite Ceramic Powders

M. Y. Shareef M. A. Hassen
Jubail Industrial College, Jubail Industrial City
K. A. Maher
College of Science, University of Zakho

(NJC)

(Received on 10/3 /2010)

(Accepted for publication 27/9/2011)

Abstract

Thermal stability and sintering behaviour of two hydroxyapatite (HAP) powders where designated. AHAP and BHAP have been investigated at fired sintering temperature range from 1100 to 1450 °C for 3 hrs using XRD and IR spectroscopy. The fired compacts have been characterised by measuring their bulk density, firing shrinkage and biaxial flexural strength (BFS).

BHAP has been found to transform to oxyhydroxyapatite (OHAP) at $T \geq 1200^{\circ}\text{C}$, and at $T \geq 1300^{\circ}\text{C}$ started to decompose to β -tricalcium phosphate (β -TCP). AHAP has been found to be marginally less stable than BHAP with OHAP forming at $T \geq 1150^{\circ}\text{C}$ and β -TCP forming at $T \geq 1200^{\circ}\text{C}$. In both materials, β -TCP transformed to α -TCP at $T \geq 1350^{\circ}\text{C}$. Maximum densification (~95% of theoretical density) occurred at a lower firing temperature for AHAP (1150°C) than for BHAP (1250°C), with AHAP also showing a slightly higher firing shrinkage (23% compared with 20% for BHAP). The BFS of both materials have been found to increase with increasing sintering temperature up to 1300°C , reaching a maximum value of ~90-100 MPa. At $T \geq 1300^{\circ}\text{C}$, this is followed by rapid reduction in BFS due to cracks forming as a result of a volume increase associated with the transformation of β -TCP into α -TCP.

It has been concluded that BHAP is marginally more thermally stable than AHAP, while the latter densifies at a lower firing temperature, this is not a disadvantage and comparable properties can be achieved for both powders, although different firing conditions need to be used.

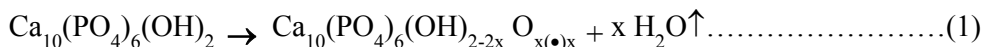
Keywords: Hydroxyapatites (HAP), Biomaterials, Oxyhydroxyapatite, Linear Shrinkage, Biaxial Flexural Strength, Densification.

(BHAP) (PAH) (AHAP)
 ° 1100 -1450 . IRS XRD .
 (OHAP) (BHAP) ° 1300 ≤ T ° 1200 ≤ T .
 (BHAP) (AHAP) .(β-TPC)
 (β-TPC) ° 1150 ≤ T (OHAP)
 ° 1350 ≤ T (α-TPC) (β-TPC) . ° 1200 ≤ T
 aP BFS
 100 – 90 ~ M

Introduction

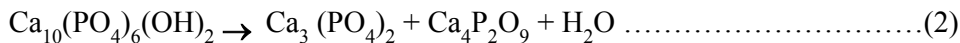
Hydroxyapatites (HAP) have been studied extensively and its biocompatibility is well recognised whether implanted in soft tissue [1-3] or hard tissue [4-7]. Its main interest is as a bone substitute, as it is considered to be bioactive in that it can form a chemical bond to the bone [8-11]. This bone bonding has also been described for other calcium phosphates, glass-ceramics, and bio-glasses [12-14].

HAP with various degrees of porosity and different strengths have been produced, using powder press, hot press, hot isostatic press and slip cast techniques [15-17]. These processing methods may alter the HAP either due to dehydroxylation or decomposition depending on the sintering temperatures. In the former process HAP loses hydroxyl groups during heating and transforms to oxyhydroxyapatite as follows [18]:



Where (•) is a vacancy, x<1. In the latter process Locardi *et al.* [19] have reported that the HAP decomposes into β-TCP or α-TCP and tetra calcium phosphate when the sintering

temperature is more than 1125°C according to the formula:



However, the temperatures at which these transformations occur are dependent on the purity of the HAP and will vary from one material to another [20]. As consequence, much of the experimental work on the biocompatibility of calcium phosphate ceramics has come into question because of inappropriate or insufficient characterization of the material [21]. Therefore, the thermal behaviour of the HAP, as it is processed, needs be known so that the characteristic properties of the final material can be assured. In this study the thermal behaviour of two sources of HAP are examined in order to assess differences in their sintering behaviour.

Materials and Methods

One material, designated AHAP, was supplied by Euro Crystals BV (Landgraaf, Holland) consisted of compact well defined agglomerates. The other material, designed BHAP, was supplied by Plasma Biotal (Tideswell, Derbs, UK) and consisted of loosely clustered, poorly defined agglomerates [17].

1. Characterisation of the powders

Particle size morphology of the starting powders was determined using SEM and TEM images as the particle size distribution was already

determined [31] using particle size analyser (Coulter LS 130) which employs a laser diffraction method.

Thermal stability of the powders was examined using infra-red spectroscopy IR and X-Ray diffraction (XRD). Samples of powder were fired in an air atmosphere for 3 hr at temperatures from 1100 to 1450 °C by 50 °C temperature intervals. Infra-red spectra for both as-received and fired powders were recorded from 200 to 4000 cm⁻¹ at ambient temperature using a Perkin-Elmer 683 infra-red spectrophotometer. Samples were pelletized with KBr at a load of 10 tonnes in an evacuated die for 10 min to minimise water adsorption. XRD examinations for both as-received and fired powders were carried out using CuK α radiation in a Philips X-ray diffractometer. A scan rate of 3^o/min was employed over the range of 10^o to 70^o for all samples to be tested. 2 θ values of the peaks were determined from the X-ray trace and calculated d-value compared with those listed in A.S.T.M powder diffraction files.

2. Fabrication and Characterisation of the Fired Samples

A single ended uniaxial steel die of 13.5 mm diameter and hand-operated hydraulic press were employed to

produce green compacts of 3 mm thickness. Compacts were formed by applying a load of 1 tonne for 1 min. It was found that higher compaction load led to fracture of the compacts during pressing. The compacts were fired at sintering temperatures ranging from 1100°C to 1450 °C in air atmosphere for 3 hr at temperature intervals of 50 °C. Ten compacts were produced for each firing condition. In addition, two compacts produced from each powder were fired at 1250 °C for 3 h in a steam atmosphere using a system described elsewhere [22].

The green and the fired compacts were weighed and their diameters and heights were measured using a micrometer (Mitutoyo, Japan). The bulk densities of the fired compacts were calculated using a geometrical method which involves dividing the weight of the compact by its bulk volume. The percentage theoretical density was calculated using the bulk density of the compacts and the theoretical density value for HAP of 3.156 g cm^{-3} [23]. The linear shrinkage values of the fired compacts were determined by measuring the initial and the fired diameters of each sample. The biaxial flexural strength was determined for 10 test-pieces of each

HAP powder using the method described previously [24].

Results and Discussions

The particles size morphology of the two starting powders is presented in Fig 1. as SEM and TEM micrographs. They clearly show that AHAP powder has tightly packed agglomerated structure while the BHAP is loosely packed. This is a confirmation of an earlier determination of the particle size distribution which showed that BHAP powder has a considerably smaller particle size distribution than the AHAP powder, with a mean particle size of $5.123 \mu\text{m}$ and $15.06 \mu\text{m}$ respectively [31].

IR spectroscopy was employed to investigate whether the dehydroxylation process occurred during firing in either air or a steam atmosphere. The complete infra-red absorption spectrum of powder AHAP is shown in Fig. 2A and is similar to that presented by Rootare *et al* [25] and that for BHAP was reported in a previous publication [17]. The presence or absence of the OH groups which are lost during dehydroxylation can be followed by a corresponding presence or absence of the OH absorption peak at 630 cm^{-1} and 3570 cm^{-1} [20]. The

latter is difficult to use since it is close to the broad peak at 3430 cm^{-1} due to adsorbed water [20, 22, 26]. Other peaks such as those at 870 and $1385\text{-}1550\text{ cm}^{-1}$ region are due to carbonate ions. These peaks disappeared as the firing temperature was progressively increased.

IR spectra for the PB are presented in Fig. 2B for the range of firing temperatures investigated. It can be seen that both materials lose their hydroxyl groups as indicated by the gradual disappearance of the OH peaks at 630 cm^{-1} . The results also show that AHAP begins to dehydroxylate at 1150°C , whereas for BHAP this occurs at the slightly higher temperature of 1200°C . This observation confirms that of other workers where temperatures for the onset of dehydroxylation have been found to vary depending on the source powder [27,28]. This transformation to OHAP is however preventable when the HAP is fired in a steam atmosphere [22] as confirmed by the retention of the 630 cm^{-1} absorption peaks. This was the same for both powders.

The XRD data for powder AHAP in the as-received state and after firing in different atmospheres are presented in Fig. 3A. This powder appears to

consist of high purity and highly crystalline HAP and shows no discernible difference to data obtained for the as-received powder BHAP presented in Fig. 3B and compared to data previously published [17]. The XRD traces of the fired materials had well defined peaks, which might be expected with the crystal growth that occurred on firing. This is well demonstrated especially as different atmosphere is used on firing Fig. 3A & 3B. Other than the dehydroxylation, which is not discernible on XRD, AHAP was stable up to 1200°C and started to decompose at temperature in excess of 1200°C when peaks attributable to $\beta\text{-TCP}$ began to appear. In contrast, BHAP is more stable and only at temperatures of 1300°C and higher do $\beta\text{-TCP}$ peaks begin to appear. For both materials, when fired at a sintering temperature of more than 1350°C , the $\beta\text{-TCP}$ disappeared and $\alpha\text{-TCP}$ formed instead, which confirms in the earlier work [22]. The thermal behaviour of both powders can be clearly seen on the TG and DTA graphs shown in Fig. 4 & 5 where changes clearly corresponds the XRD patterns seen.

The % theoretical density, % linear firing shrinkage of both AHAP and

BHAP were plotted as a function of sintering temperature as shown in Figs. 6 and 7 respectively. Both material became more dense as the sintering temperature increased from 1100°C to 1450°C, achieving approximately 95% of theoretical density at temperature in excess of 1300°C. A major difference was observed in the rate of densification with AHAP densifying much more rapidly than BHAP at the lower temperatures, with a corresponding higher degree of linear shrinkage. This behaviour of densification, which may be seen as contrary to expectation when considering the particle size distribution, is due to the non-uniformities of the particle size distribution, porosity and particle alignment of the green compacts [22,23]. Nevertheless, even at the higher temperatures the AHAP powder achieved a slightly higher theoretical density than BHAP and also a higher linear shrinkage.

The biaxial flexural strength of both HAP materials were plotted against sintering temperature are presented in Fig. 8. As might be expected from the increased density with higher firing temperature, the biaxial flexural strength increased with increasing

sintering temperature up to 1300°C. The maximum biaxial flexural strength values obtained were 100 MPa and 93 MPa for AHAP and BHAP respectively. As the sintering temperature is increased a more dense material resulted and consequently a higher biaxial flexural strength was achieved for both materials. AHAP reached its maximum BFS at 1150°C whereas BHAP did not achieve its maximum until 1300°C, just as it reaches its decomposition temperature. This difference is due to the rapid densification of AHAP compared with BHAP. The slightly higher value for the BFS of AHAP can be explained by virtue of its slightly higher density. Above 1300°C, the biaxial flexural strength of both materials reduced rapidly, although the % theoretical density was relatively unaffected. The reason for this is that the transformation of HAP into α -TCP produces a volume increase, which causes cracking on the surface and reacts as a flaw-initiating fracture [30,31].

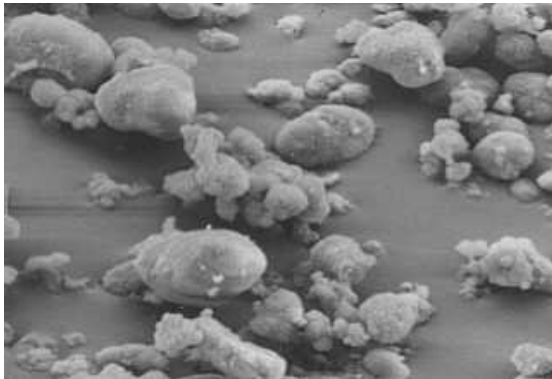
The dehydroxylation had no effect on the BFS and since it also cannot be monitored by XRD, it is important that IRS is used whenever HAP is to be

characterised prior to high temperature processing.

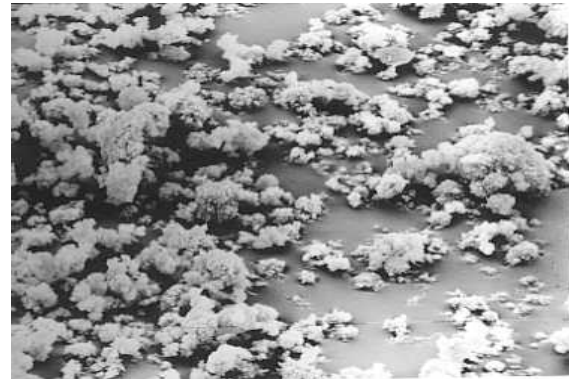
Conclusions

The thermal behaviour of two types of hydroxyapatites-HAP ceramic powders designated as AHAP & BHAP was studied. BHAP is more resistant to dehydroxylation than AHAP whereas powder AHAP shows a more rapid

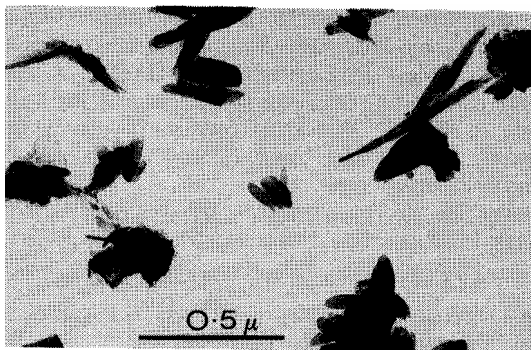
densification than powder BHAP, especially at sintering temperatures less than 1200 °C. The dehydroxylation did not affect the biaxial flexural strength of either powder. The transformation of HAP to α -TCP causes a substantial loss of biaxial flexural strength.



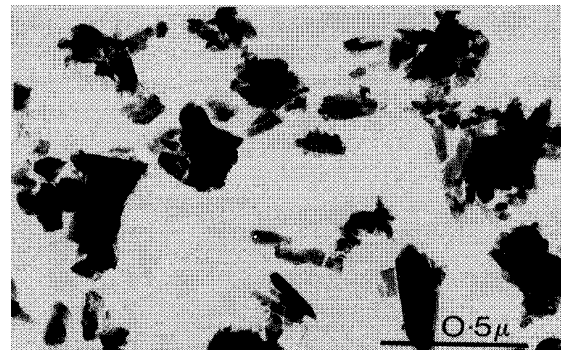
SEM Micrograph of Powder AHAP (mag. $\times 1250$)



SEM Micrograph of Powder BHAP (mag. $\times 1250$)

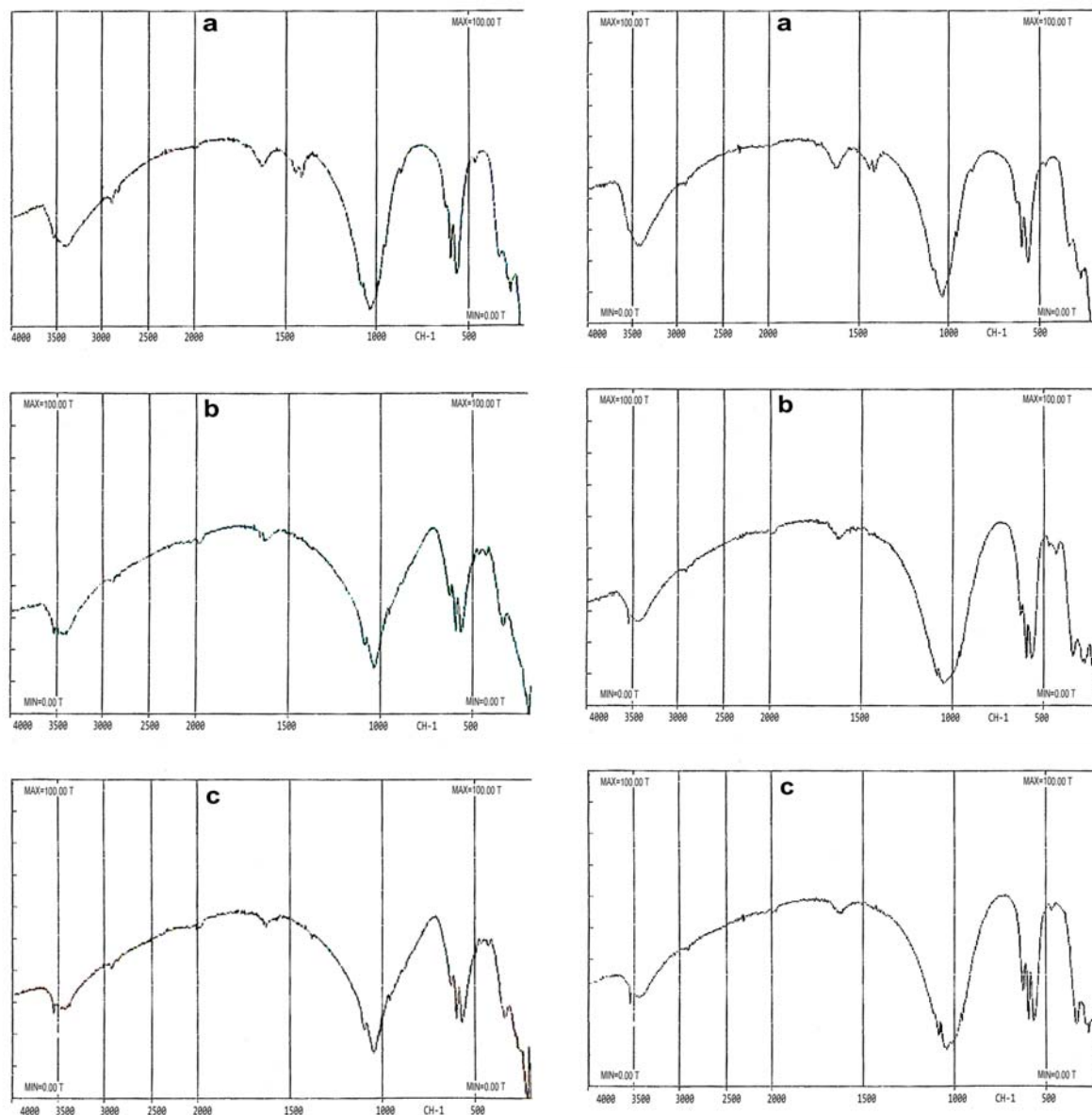


TEM Micrograph of Powder AHAP



TEM Micrograph of Powder BHAP

Figure 1: The morphology of powders AHAP and BHAP as received.



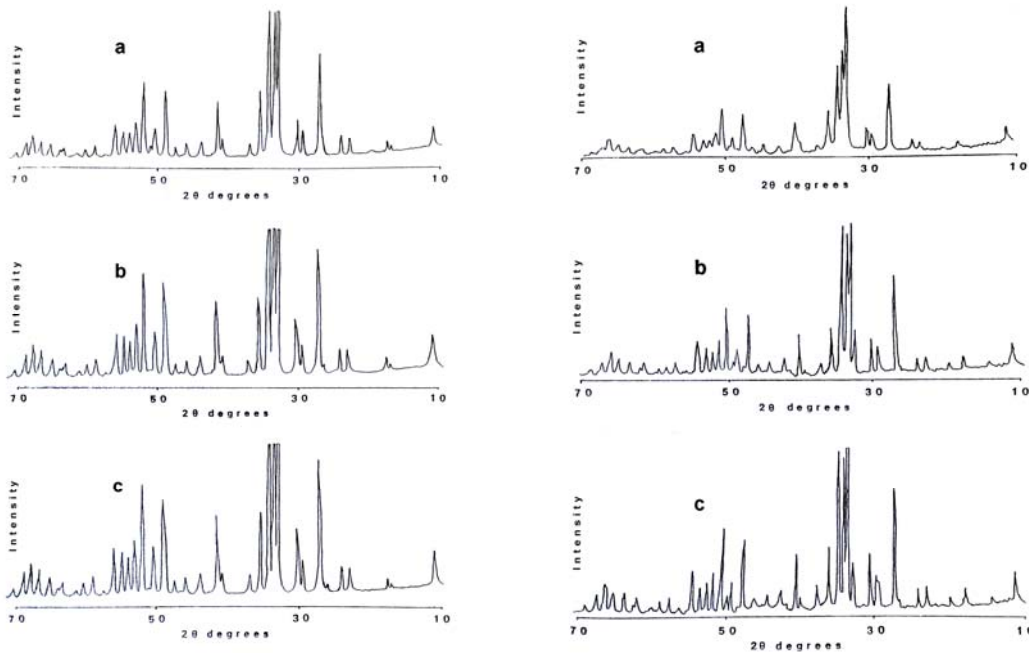
(A) IR Absorption Spectrum for AHAP Powder

(a) as received, (b) fired at 1200°C, (c) fired at
1300°C

(B) IR Absorption Spectrum for BHAP Powder

(a) as received, (b) fired at 1200°C, (c) fired at
1300°C

Figure 2: IR absorption spectrum for (A) AHAP powder, (B) BHAP powder.



(A) XRD Traces of Powder AHAP, (a) as received, (b) fired at steam/nitrogen atmosphere and (c) fired at air atmosphere

(B) XRD Traces of Powder BHAP, (a) as received, (b) fired at steam/nitrogen atmosphere and (c) fired at air atmosphere

Figure 3: XRD traces for (A) AHAP powder, (B) BHAP powder fired at different atmospheres.

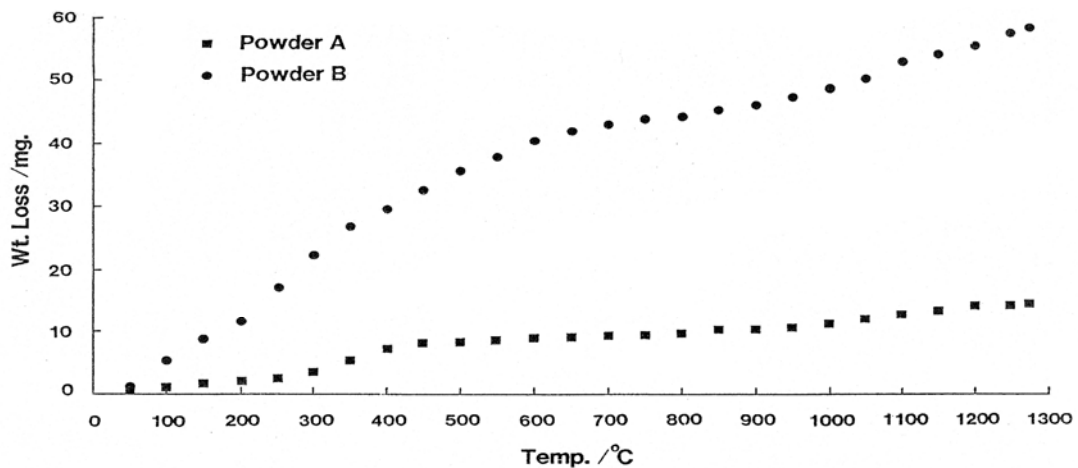


Figure 4: TG curves for powder AHAP as A and powder BHAP as B.

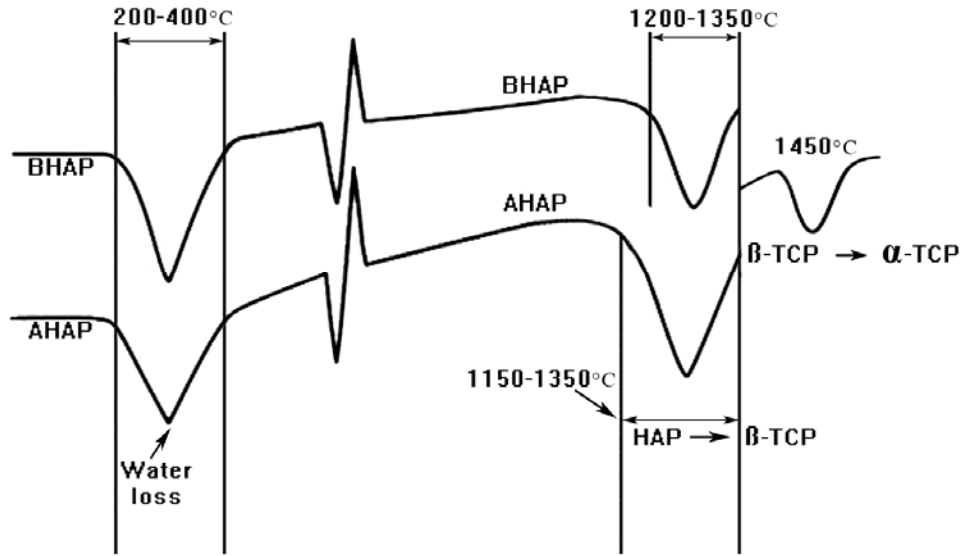


Figure 5: DTA graph for powders AHAP and BHAP.

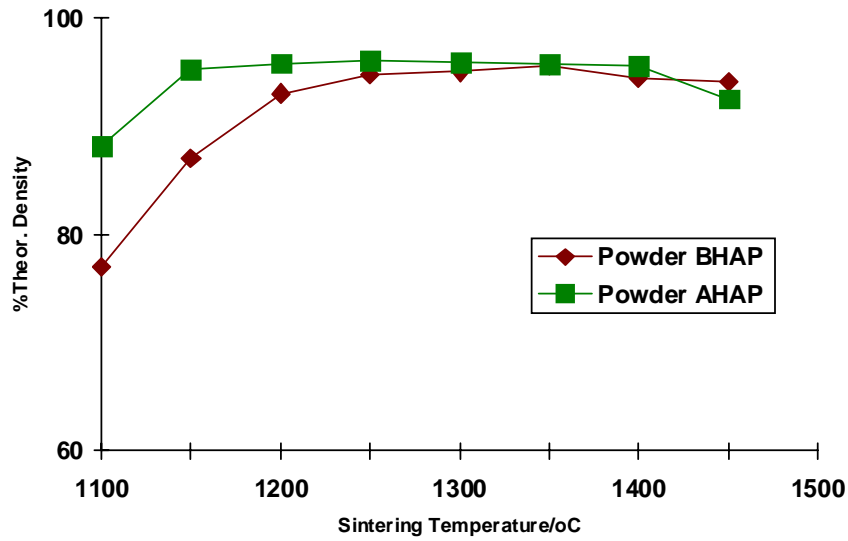


Figure 6: Theoretical density at different sintering temperatures.

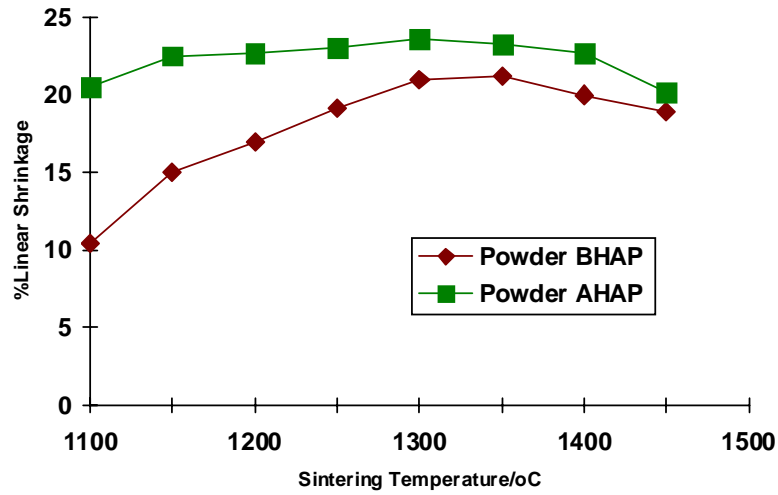


Figure 7: Percentage of linear shrinkage at different sintering temperatures.

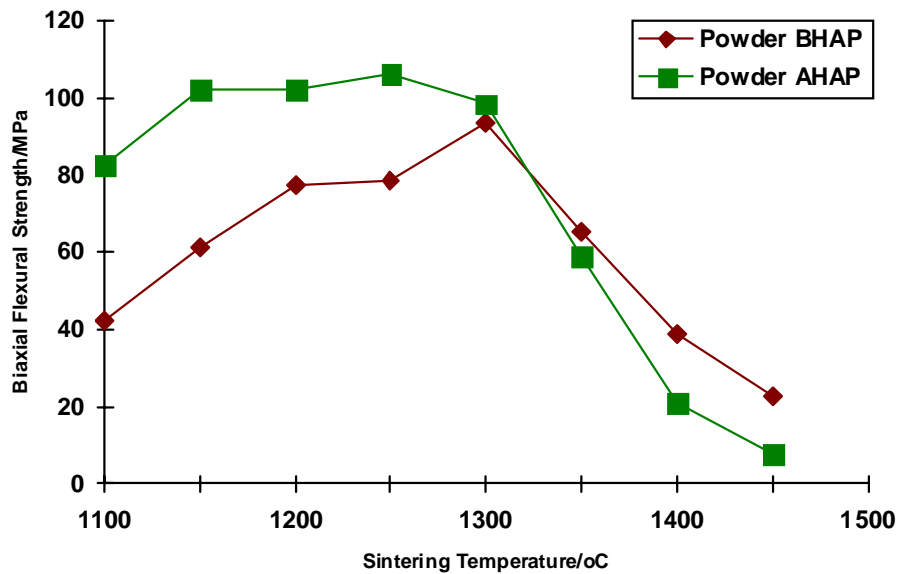


Figure 8: The Biaxial Flexural Strength of both HAP powders at different sintering temperature.

References

1. (a) M. P. MAHABOLE, R. C. AIYER, C. V. RAMAKRISHNA, B. SPREEDHAR and R. S. KHAIRNAR, *Bull. Mater. Sci.*; 2005, **28-6**, 535.
M. OGISO, H. KANEDA, J. ARASAKI and T. TABATA, in "Biomaterials 1980", (b) G.D.WINTER, D.F.GIBBONS and H.PLENCK (Eds), (John Wiley & Sons, Ltd., London, 1982) p 59.
2. J. A. JANSEN, J. R. de WIJN, J. M. L. WOLTERS-LUTGERHORST and P. J. van MULLEM, *J. Dent. Res.*; 1985, **64**, 891.
3. C. A. van BLITTERSWIJK, S. C. HESSELING, J. J. GROTE, H. K. KOERTEN and K. de GROOT, *J. Biomed. Mater. Res.* 1990, **24**, 433.
4. M. JARCHO, J. F. KAY, I. KENNETH, K. I. GUMAER, R. H. DOREMUS and H. P. DROBECK, *J. Bioeng.* 1977, **1**, 79.
5. H. W. DENISSEN, K. de GROOT, P. C. H. MAKKES, A. van den HOOFF and P. J. KLOPPER, *J. Biomed. Mater. Res.*; 1980, **14**, 713.
6. K. de GROOT, in "Bioceramics of calcium phosphates" K. de GROOT (Ed), (CRC Press, Boca Raton, FL, USA, 1983) p 100.
7. C. A. van BLITTERSWIJK, J. J. GROTE, W. KUIJPERS, C. J. G. BLOK-van HOEK and W. Th. DAEMS, *Biomaterials*, 1985, **6**, 243.
8. M. JARCHO, *Clin. Orthop. Relat. Res.*; 1981, **157**, 259.
9. J. F. OSBORN and H. NEWSELY, in "Biomaterials 1980", G.D.WINTER, D.F.GIBBONS and H.PLENCK (Eds), (John Wiley & Sons, New York, 1980) p 51.
10. T. FUJII and M. OGINO, *J. Biomed. Mater. Res.*; 1984, **18**, 845.
11. L. L. HENCH and J. WILSON, *Science*; 1984, **226**, 630.
12. L. L. HENCH, R. J. SPLINTER, W. C. ALLEN and T. K. GREENLEE, *J. Biomed. Mater. Res. Symp.*; 1971, **2**, 117.
13. L. L. HENCH and H. A. PASCHALL, *J. Biomed. Mater. Res. Symp.*; 1974, **5**, 49.
14. U. M. GROSS, J. BRANDES, V. STRUNZ, I. BAB and J. SELA, *J. Biomed. Mater. Res.*; 1981, **15**, 291.
15. H. DENISSEN, C. MANGANO and G. VENINI, "Hydroxyapatite implants" (Piccin Nuova Libreria, SPA, Padua, 1985) p 19.
16. M. WINTER, P. GRISS, K. DE GROOT, H. TAGAI, G. DIJK HEIMKE, and K. SAWAI, *Biomaterials*, 1981, **2**, 159.
17. M. Y. SHAREEF, P. F. MESSER, and R. van OORT, *Biomaterials.*; 1993, **14**, 69.
18. C. LAVERNIA and J. M. SCHOENUNG, *Ceram. Bull.*; 1991, **70**, 95.
19. B. LOCARDI, U. E. PAZZAGLIA, C. GABBI and B. PROFILO, *Biomaterials* (1993) **14** 437.
20. Z. JIMING, Z. XINGDONG, C. JIYONG, Z. SHAOXIAN and K.

- de GROOT, *J. Mater. Sci. Materials in Medicine.*;1993,**4**, 83.
21. Z. RACQUEL and Le GEROS, *Clinical Material.*;1993,**14**,65.
22. M. Y. SHAREEF, P. F. MESSER, and R. van NOORT, *Br. Ceram. Proc.*; 1990,**45**, 59.
23. M. Y. SHAREEF, P. F. MESSER and R. van NOORT, *Br. Ceram. Proc.* special Ceramics ;1992,**49**, 121.
24. M.Y.SHAREEF, R. van NOORT, P.F.MESSER and V.PIDDOCK, *J. Mater. Sci. Materials in Medicine* ;1994,**5**,113.
25. H. M. ROOTARE, J. M. POWERS and R. G. GRAIG, *J. Dent. Res.*;1978,**57**,777.
26. Infra-red Spectra of Adsorption Species, Edt. by L.H., Little, *Academic Press. Inc. Ltd.* London, 1966.
27. C. REY, M. FRECHE, M. HEUGHEBAERT, J. C. HEUGHEBAERT, J. L. LACOUT, A. LEBUGLE, J. SZILAGYI and M. VIGNOLES, in Bioceramics Proceedings of the 4th International Symposium on ceramics in Medicine, Vol. **4** Edited by W. Bonfield, G.W. Hasting and K.E. Tanner (Butterworth-Heinemann Ltd., 1991) p 56.
28. J. D. SANTOS, S. MORREY, G. W. HASTINGS and F. G. MONTEIRO, in Bioceramics Proceedings of the 4th International Symposium on Ceramics in Medicine, Vol. 4 W.BONFIELD, G.W.HASTING and K.E.TANNER (Eds.) (Butterworth-Heinemann Ltd., 1991) p 71.
29. D. GREEN, *J. Amer. Ceram. Soc.*;1983, **66**, 807.
30. A. ROYER, J. C. VIGUIE, M. HEUGHEBAERT and J. C. HEUGHEBAERT, *J. Mater. Sci. Materials in Medicine.*;1993, **4**,76.
31. M. K. Hilal, Ph.D Thesis, The University of Sheffield, 1996.